

# Resistance factor calibration for perforated cold-formed steel compression members

## Calibración del factor de resistencia a la compresión en perfiles de acero conformado en frío perforados

Roberta Layra Faragó Jardim <sup>1\*</sup> <http://orcid.org/0000-0003-2350-1038>, Marcilio Sousa da Rocha Freitas \* <http://orcid.org/0000-0003-4664-5368>, André Luís Riqueira Brandão\*\* <http://orcid.org/0000-0002-4857-4308>

\*Federal University of Ouro Preto, Ouro Preto - Brasil

\*\*Federal University of Itajubá / Itabira, Itabira - Brasil

Fecha de Recepción: 16/08/2021

Fecha de Aceptación: 29/12/2021

PAG 35-46

### Abstract

*Cold-formed Steel profiles are structural profiles widely used in civil construction. They are often manufactured with perforations. The designing can be performed using the direct resistance method. Formulations were adapted by Moen and Schafer (2008) to consider the presence of perforations in these profiles. The objective of this study is to investigate the structural safety of columns with web perforations. The calculation of the resistance capacity was performed using the formulations proposed by the authors. The reliability indexes were determined using the First Order Reliability Method (FORM), First Order Second Moment (FOSM) and Monte Carlo Method (MCM), which are reliability methods for the Load and Resistance Factor Design (LRFD) and Limit States Design (LSD) philosophies. Following the same criteria performed by AISI S100, the resistance factors were obtained from the FOSM method. Based on the results, it was found that the desired security level for the LSD philosophy was not achieved. The calculated resistance factors are predominantly lower than the target. However, for the LRFD philosophy, the safety level was achieved, and the resistance factors were higher than the target.*

*Keywords: Reliability, cold-formed steel, holes, DSM, compression*

### Resumen

Los perfiles de acero conformados en frío son perfiles estructurales muy utilizados en la construcción civil, comúnmente fabricados con perforaciones. El diseño se puede realizar utilizando el método de resistencia directa. Las formulaciones fueron adaptadas por Moen y Schafer (2008), las cuales consideran la presencia de perforaciones. El objetivo de este estudio es investigar la seguridad estructural de columnas con perforaciones en el alma. El cálculo de la capacidad de resistencia se realizó utilizando las formulaciones propuestas por los autores mencionados. Los índices de confiabilidad se determinaron utilizando el Método de Confiabilidad de Primer Orden (FORM), de Primer Orden Segundo Momento (FOSM) y el Método de Montecarlo, que son métodos de confiabilidad para los Factores de Carga y de Resistencia (LRFD) y Estados Límite (LSD). Siguiendo los mismos criterios realizados por el AISI S100, los factores de resistencia se obtuvieron del método FOSM. Con base en los resultados, se encontró que no se logró el nivel de seguridad deseado para la filosofía LSD. Los factores de resistencia calculados son predominantemente más bajos que el objetivo. Sin embargo, para la filosofía LRFD, se logró el nivel de seguridad y los factores de resistencia fueron más altos que el objetivo.

**Palabras clave:** Fiabilidad, acero conformado en frío, perforación, método de resistencia directa, compresión

## 1. Introduction

*Cold-formed Steel (CFS) profiles have less weight and greater width / thickness ratio plates. For this reason, section instabilities and instabilities along the length of the profiles can occur. Among the existing procedures for dimensioning CFS profiles, the Direct Strength Method (DSM) stands out. This is a method originally developed by (Schafer and Pekoz, 1998), whose resistance calculation is based on analyses of elastic buckling and stands out for its ease and functionality. CFS profiles have commonly been manufactured with perforations along their length, on flanges and webs. The perforations permit the accommodation and passage of pipes in the walls and ceilings of the buildings, in addition to the connection between construction profiles. Several sections can be manufactured from CFS members, providing advantages for their use. This study gathered profiles with perforated lipped C-section type, but studies have been developed with other perforated sections, such as rack profiles and closed profiles, due to the importance and use of these components in other construction systems. The existing demand for profiles with perforations has led to studies by (Moen and Schafer, 2008), who presented proposals for changes to the original DSM buckling curves.*

<sup>1</sup> **Corresponding author:**

Federal University of Ouro Preto, Ouro Preto - Brasil

E-mail: roberta.farago@hotmail.com



The United States, Mexico and Canada use the North American standard (North American Specification - NAS) for the design of steel structures consisting of CFS sections. The North American standard includes design provisions for LRFD (Load and Resistance Factor Design), used by the United States and Mexico, and LSD (Limit States Design), used in Canada (AISI, 2016).

A limit state is represented as a condition for which a structural member or structural system fails to perform the function for which it was designed (Hsiao, 1989). For the limit state of resistance, the usual format of the LRFD method is represented by (Equation 1). LSD and LRFD are based on the same philosophy: the design load effect does not exceed the design resistance.

$$\sum \gamma_i Q_i \leq \phi R_n \quad (1)$$

where  $R_n$  is the nominal resistance,  $\phi$  is the resistance factor,  $\gamma_i$  is the load factor and  $Q_i$  is the load effect.  $R_n$  is obtained based on an appropriate analytical model, using the properties of the nominal section and the specified minimum material properties. The resistance factor involves the uncertainties and variability inherent in the nominal resistance. The load factor involves the uncertainties and variability of the loads and the effects of the load (Ellingwood et al., 1980).

In the LRFD and LSD formats, structural reliability is characterized in terms of a reliability index,  $\beta$ , determined by a statistical analysis of loads and resistances. Load and resistance factors are obtained so that the reliability of a structure is at the desired level, using the proposed normative provisions. The reliability index is related directly to the load and resistance factors used in the project, and consequently, to the structural reliability of the project. The technical committee responsible for developing the design standards must calibrate the resistance factors, so that the reliability index reaches a required target value  $\beta_0$ .

A reliability method aims to assess a reliability index or a probability of failure. When the method is used in standard calibration, resistance factors are proposed so that the calculated reliability indexes approximate an established target reliability index  $\beta_0$ . Procedures for calibrating the first standards in limit states (Ravindra and Galambos, 1978); (Ellingwood et al., 1980); (Hsiao, 1989), are still used in the structural verification of propositions for new design equations, or adaptations that may result in updating standards.

For the North American specification, the resistance factors  $\phi = 0.85$  (LRFD) and  $\phi = 0.80$  (LSD), for CFS steel members under compression, were calibrated with FOSM (Hsiao, 1989). The calibration data for LRFD has the following values for the nominal live-to-dead load ratio ( $L_n/D_n$ ), the load combinations and the target reliability index:  $L_n/D_n = 5$ ,  $1.2D_n + 1.6L_n$ , and  $\beta_0 = 2.5$ . Likewise, the LSD calibration data are:  $L_n/D_n = 3$ ,  $1.25D_n + 1.5L_n$ , and  $\beta_0 = 3.0$ .

The resistance factor can be calculated by (Equation 2). This equation, available in the North American specification, was deduced by the FOSM method.

$$\phi = C_\theta (M_m F_m P_m) e^{-\beta_0 \sqrt{V_M^2 + V_F^2 + C_p V_P^2 + V_Q^2}} \quad (2)$$

$C_\theta$  = calibration coefficient (1.52 for LRFD; 1.42 for LSD);

$M_m$  = mean value of material factor  $M$ ;

$F_m$  = mean value of fabrication factor  $F$ ;

$P_m$  = mean value of professional factor  $P$ ;

$V_M$  = coefficient of variation of material factor  $M$ ;

$V_F$  = coefficient of variation of fabrication factor  $F$ ;

$V_P$  = coefficient of variation of professional factor  $P$ ;

$V_Q$  = coefficient of variation of load effect;

$C_p$  = correction factor (for a large number of tests  $C_p$  close to 1).

The basis of the project for the LRFD and LSD formats is the same. However, the values of the target reliability index, as well as the load ratio are different for each design philosophy. As the calibration coefficient depends mainly on the  $L_n/D_n$  ratio and the load combination, different values are obtained for LRFD and LSD, so that  $C_\theta$  is 1.52 for LRFD and 1.42 for LSD.

The objective of this article is to evaluate the reliability of members in cold-formed, perforated web profiles submitted to axial compression force. The resistance calculation followed criteria proposed by (Moen and Schafer, 2008), based on a database with 183 columns. The values for the professional factor calculated in this study were obtained from the ratio between the experimental results of the database and the calculated theoretical results. To obtain the reliability indexes, the following reliability methods were employed: FOSM - First Order Second Moment,



FORM - First Order Reliability Method and the Monte Carlo Method (MCM). The same calibration data as the American standard was used. The results obtained were compared with the target indexes of the LRFD and LSD design philosophies. The resistance factors were calibrated using the FOSM reliability method.

## 2. Methodology

### 2.1 The Direct Strength Method

The Direct Strength Method can be used to obtain axial compressive forces in cold-formed profiles. This is a method that uses properties of elastic buckling to calculate resistance (Toledo, 2021). To identify the buckling modes and their respective critical loads, software based on the finite strip method can be used, such as the CUFSM (Constrained and Unconstrained Finite Strip Method) adopted in this study. Formulations for global ( $P_{ne}$ ), local ( $P_{nl}$ ) and distortional ( $P_{nd}$ ) buckling, without perforations, are shown below.

#### Global

$$P_{ne} = (0.658\lambda_c^2)P_y \quad \text{for } \lambda_c \leq 1.5 \quad (3)$$

$$P_{ne} = \left(\frac{0.877}{\lambda_c^2}\right)P_y \quad \text{for } \lambda_c > 1.5 \quad (4)$$

Where:

$$\lambda_c = \left(\frac{P_y}{P_{cre}}\right)^{0.5}$$

$\lambda_c$  is the slenderness factor of global buckling for column;

$P_y$  is yield load;

$P_{cre}$  is the global buckling.

#### Local

$$P_{nl} = P_{ne} \quad \text{for } \lambda_l \leq 0.776 \quad (5)$$

$$P_{nl} = \left[1 - 0.15 \left(\frac{P_{crl}}{P_{ne}}\right)^{0.4}\right] \left(\frac{P_{crl}}{P_{ne}}\right)^{0.4} P_{ne} \quad \text{for } \lambda_l > 0.776 \quad (6)$$

Where:

$$\lambda_l = \left(\frac{P_{ne}}{P_{crl}}\right)^{0.5}$$

$\lambda_l$  is the slenderness factor of local buckling for column;

$P_{crl}$  is the local buckling force.



## Distortional

$$P_{nd} = P_y \quad \text{for } \lambda_d \leq 0.561 \quad (7)$$

$$P_{nd} = \left[ 1 - 0.25 \left( \frac{P_{crd}}{P_y} \right)^{0.6} \right] \left( \frac{P_{crd}}{P_y} \right)^{0.6} P_y \quad \text{for } \lambda_d > 0.561 \quad (8)$$

Where:

$$\lambda_d = \left( \frac{P_y}{P_{crd}} \right)^{0.5}$$

$\lambda_d$  is the slenderness factor of distortional buckling for column;  
 $P_{crd}$  is the distortional buckling force.

The extension of DSM to columns with perforations was performed based on adaptations of the formulations of the original method presented. (Moen and Schafer, 2008) developed 6 modifications, but only four formulation options were evaluated in this study: DSM 2, DSM 3, DSM 4, DSM 5. In all options developed by the authors, the influence of the perforations should be considered in determining the global ( $P_{cre}$ ) local ( $P_{cr\ell}$ ) and distortional ( $P_{crd}$ ) elastic buckling force in compression.

DSM 1 - The original MRD equations for obtaining  $P_{ne}$ ,  $P_{n\ell}$  and  $P_{nd}$  (AISI S100) are normally applied, but the influence of the perforation is considered in the buckling analysis.

DSM 2 - The flow yield force  $P_y$  of the original MRD equations is replaced by the flow force  $P_{ynet}$ , obtained with the cross section in the region of the perforation (net cross-section).

DSM 3 - The nominal axial strengths  $P_{n\ell}$  and  $P_{nd}$  are limited to member yield strength on net cross-section  $P_{ynet}$ .

DSM 4 - In this formulation,  $P_{ne}$  and  $P_{n\ell}$  follow the original formulation, but  $P_{n\ell}$  is limited to  $P_{ynet}$ . In addition, in the original for obtaining the nominal axial strength for distortional buckling ( $P_{nd}$ ) a modification starts to consider a transition between the elastic buckling and the yielding at the net cross-section.

$$P_{nd} = P_{ynet}, \quad \text{for } \lambda_d \leq \lambda_{d1} \quad (9)$$

$$P_{nd} = P_{ynet} - \left( \frac{P_{ynet} - P_{d2}}{\lambda_{d2} - \lambda_{d1}} \right) (\lambda_d - \lambda_{d1}), \quad \text{for } \lambda_{d1} \leq \lambda_d \leq \lambda_{d2} \quad (10)$$

$$P_{nd} = \left[ 1 - 0.25 \left( \frac{P_{crd}}{P_y} \right)^{0.6} \right] \left( \frac{P_{crd}}{P_y} \right)^{0.6} P_y, \quad \text{for } \lambda_d > \lambda_{d2} \quad (11)$$

$$P_y = A_g F_y \quad (12)$$

$$\lambda_{d1} = 0.561 \left( \frac{P_{ynet}}{P_y} \right) \quad (13)$$

$$\lambda_{d2} = 0.561 \left[ 14 \left( \frac{P_{ynet}}{P_y} \right)^{-0.4} - 13 \right] \quad (14)$$



$$P_{d2} = \left[ 1 - (1 - 0.5\lambda_{d2}^{-1.2})^2 \right] P_y \quad (15)$$

$$P_{ynet} = A_{net}F_y \geq 0.6P_y \quad (16)$$

Where:

$$\lambda_d = \left( \frac{P_y}{P_{crd}} \right)^{0.5}$$

$\lambda_{dnet}$  is the reduced slenderness factor of the perforated section associated with the distortional buckling;

$A_g$  is the gross area of the cross-section of the column;

$A_{net}$  is the net area of the cross-section of the column;

$F_y$  is the yield stress of the material;

$P_{crd}$  is the critical axial bending force of the perforated profile;

$P_{nd}$  is the characteristic compressive strength of the perforated profile, associated with distortional buckling.

DSM 5 - The same transition defined for DSM 4 is considered in the distortional buckling. In addition, a transition was introduced in the formulation of local buckling, from  $P_{nl}$  to  $P_{ynet}$ .

$$P_{nl} = P_{ne} \leq P_{ynet}, \text{ for } \lambda_l \leq \lambda_{l1} \quad (17)$$

$$P_{nl} = P_{ynet} - \left( \frac{P_{ynet} - P_{l2}}{\lambda_{l2} - \lambda_{l1}} \right) (\lambda_l - \lambda_{l1}),$$

$$\text{for } \lambda_{l1} \leq \lambda_l \leq \lambda_{l2} \quad (18)$$

$$P_{nd} = \left[ 1 - 0.25 \left( \frac{P_{crd}}{P_y} \right)^{0.6} \right] \left( \frac{P_{crd}}{P_y} \right)^{0.6} P_y$$

$$\text{for } \lambda_{l1} \leq \lambda_l \leq \lambda_{l2} \quad (19)$$

$$P_{nl} = \left[ 1 - 0.15 \left( \frac{P_{crl}}{P_{ne}} \right)^{0.4} \right] \left( \frac{P_{crl}}{P_{ne}} \right)^{0.4} P_{ne}, \quad (20)$$

$$\lambda_{l2} = 0.776 \left[ 1.7 \left( \frac{P_{ynet}}{P_{ne}} \right)^{-1.6} - 0.7 \right],$$

$$\frac{P_{ynet}}{P_{ne}} \leq 1 \text{ or } \lambda_{l2} = 0.776, \frac{P_{ynet}}{P_{ne}} > 1 \quad (21)$$

$$P_{l2} = [1 - 0.15(\lambda_{l2})^{-0.8}](\lambda_{l2})^{-0.8} P_{ne} \quad (22)$$

$$P_y = A_g F_y \text{ and } P_{ynet} = A_{net} F_y \geq 0.6 P_y \quad (23)$$

Where:

$$\lambda_l = \left( \frac{P_{ne}}{P_{crl}} \right)^{0.5}$$

$P_{crl}$  is the critical axial force of the local buckling for of perforated profiles

DSM 6 - The same transition defined for DSM 4 is considered in the distortional buckling. A transition in the formulation of the local buckling is also considered, but with a modified formulation in relation to DSM 5.



## 2.2 The FOSM, FORM and SMC Methods

Structural reliability is assessed by the relationship between the measures of failure probability,  $P_f$ , and the reliability index (Ditlevsen and Madsen, 2007) and can be resolved using approximating analytical methods (FORM and FOSM) and simulation methods, like MCM. FOSM is based on the first-order Taylor series approach and the required statistical parameters are the mean and standard deviations. The AISI S100 standard uses the FOSM to calibrate the resistance factors in force. FORM was initially proposed by (Hasofer and Lind, 1974). It is applied in a standardized normal space whose random variables are uncorrelated. For nonlinear functions, the design point determination is a nonlinear minimization constraint problem. Optimization techniques that aim to determine the design point include the Rackwitz and Fiessler method 1978. Formulations to transform the distributions of random variables into normal distributions are also presented by the authors.

The analysis carried out by the Monte Carlo Method (MCM) generates random numbers, based on their respective probability distributions. The evaluation of the structural response is given from the probability of failure, calculated by the ratio between the number of trials  $n$  for which the limit-state function is less than zero and the total number of simulations (Melchers and Beck, 2018).

## 2.3 Performance function

The safety condition for each ultimate limit state is expressed by the inequality that relates the nominal values of resistance ( $R_n$ ) and load effect ( $Q_n$ ), such that:

$$\phi R_n = \gamma_D D_n + \gamma_L L_n \quad (24)$$

$R_n$  is calculated by design formulation,  $\phi$  is the resistance factor, whose numerical value depends on the limit state under analysis and type of load effect that the member is requested,  $\gamma_D$  and  $\gamma_L$  are the load factors of the permanent and variable actions taken in the (AISI S100, 2016) and  $D_n$  and  $L_n$  are, respectively, the nominal values of dead and live loads.

Limit states are often represented mathematically by a failure function, generically described by the expression  $G(R, Q) = R - Q$ . The strength ( $R$ ) of a structural member is a function of the strength of the material, the geometry of the section and its dimensions. The request ( $Q$ ) can be expressed in terms of dead and live loads, resulting from use and occupation. The function that mathematically describes  $G(\cdot)$ , called the limit state function, is given in this study by:

$$G(\cdot) = R_n MFP - c(D + L) \quad (25)$$

Where  $M$ ,  $F$  and  $P$  are dimensionless random variables that reflect the uncertainties of the material properties, the geometry of the cross section and the design hypotheses. The random variable  $M$  is called a "material factor", determined by the ratio of a tested mechanical property and a nominal value. It is considered a random variable due to the variability inherent in the mechanical properties of the material. The "fabrication factor"  $F$  is a random variable related to the variability of geometric properties. The "professional factor"  $P$  (or model error) is a random variable that reflects the uncertainties arising from the analysis methods used.  $c$  is deterministic coefficient that relates load intensities to the loads effects. With reference to gravitational actions,  $D$  and  $L$  are the random variables of permanent and variable actions (Hsiao, 1989). The statistical parameters of the variables are shown in (Table 1) and were obtained from (Ellingwood et al., 1980). In reliability studies, it is usual to use the coefficient of variation, a measure of the dispersion of the variable in relation to the average value, in the analyses performed (Freitas et al., 2018).

Table 1. Statistical parameters of resistance and stress

Random Variable	Mean Value / Nominal Value	Coefficient of Variation	Probability Distribution Function
$M$	1.10	0.10	Lognormal
$F$	1.00	0.05	Lognormal
$D$	1.05	0.10	Normal
$L$	1.00	0.25	Gumbel



It should be noted that the reconstruction of variables  $D$  and  $L$ , in the context of the failure function, depends not only on the statistical information in (Table 1), but also on the nominal values  $D_n$  and  $L_n$ . In this case, a generic value of the nominal resistance, an  $L_n/D_n$  ratio, and a combination of ultimate normal actions are established. Then, a load factor is proposed and the security level for the established situation is obtained.

The (AISI, 2016) standard covers two design philosophies in limit states, the LRFD and the LSD. FOSM was the reliability method used for the calibration of the (AISI, 2016), but the calibration data, the resistance factors, the combinations of actions, the  $L_n/D_n$  ratio, and the target reliability indexes,  $\beta_0$ , were specific to each design philosophy. (Table 2) shows the data used for the calibration of the (AISI, 2016) standard.

Table 2. Calibration data

Type	$\gamma_D D_n + \gamma_L L_n$	$L_n/D_n$	$\phi$	$\beta_0$
LRFD	$1.2D_n + 1.6L_n$	5	0.85	2.5
LSD	$1.25D_n + 1.5L_n$	3	0.8	3.0

## 2.4 Professional Factor

The professional factor,  $P$ , is a random variable, whose analysis includes the uncertainties inherent in the model. It is the ratio between results obtained experimentally and theoretical results. The  $P$  factor provides information about the real performance of the model studied, revealing how conservative or insecure it is. In this case, the experimental values correspond to values of resistance of column tests, obtained from studies of several authors. The theoretical values were obtained from the calculation of resistances by the formulations of (Moen and Schafer, 2008) presented above.

A total of 183 tests performed by different authors were used in this study. Cold-formed lipped channel member with perforations in the webs were subjected to centered compression. The database provides a wide range of lengths and dimensions for sections and perforations. The perforations have rectangular, circular, square, or oblong shapes. Information about the database is shown in (Table 3).

Table 3. Database

Reference (year)	Profile Length (mm)	Perforation Type	$h_{hole}/b_w$	$Q_{Total}$
Ortiz-Colberg (1981)	685.8 – 1600.2	Circular	0.14 – 0.43	18
Ortiz-Colberg (1981)	304.8	Circular	0.14 – 0.50	8
Pu, Godley, Beale and Lau (1999)	356.6 – 370.1	Square	0.18 – 0.36	33
Sivakumaran (1987)	198.1 – 262.6	Various	0.18 – 0.67	39
Moen and Schafer (2008)	612.1 – 1225.6	Oblong	0.25 – 0.42	12
Miller and Pekoz (1994)	137.2 – 541.0	Rectangular	0.26 – 0.45	20
Abdel-Rahman and Sivakumaran (1998)	247.7 – 470.7	Various	0.31 – 0.38	8
Yao, Guo and Nie (2016)	797.0 – 807.0	Circular	0.13 – 0.15	18
Xu, Shi and Yang (2014)	490.0	Oblong	0.25	15
Yao (2017)	795.0 – 815.0	Oblong	0.14 – 0.15	12

The  $P$  values were calculated, the mean parameters ( $P_m$ ), standard deviation ( $\sigma_p$ ) and coefficient of variation ( $V_p$ ) were determined. The  $P$  calculations were grouped based on the failure modes obtained and the (Moen and Schafer, 2008) formulations: DSM 2, DSM 3, DSM 4 and DSM 5. The results are shown in (Table 4).



The best-fitting probability density functions (pdf) were determined using the Minitab software and Anderson-Darling fit tests. Analyses of the statistical parameters of the variable  $P$ , carried out by (Moen and Schafer, 2011), demonstrated that the methodology used in DSM 4 resulted in the best performance.

**Table 4.** Statistical parameters of the  $P$  variable.

<b>Data Group</b>	<b>Nomenclature</b>	<b>Number</b>	<b><math>P_m</math></b>	<b><math>S_P</math></b>	<b><math>V_P</math></b>	<b>pdf adjusted</b>
<b>DSM 2; Global Mode</b>	G2	14	1.074	0.120	0.112	Normal (N)
<b>DSM 2; Local Mode</b>	L2	153	1.153	0.156	0.136	Normal (N)
<b>DSM 2; Distortional Mode</b>	D2	16	1.214	0.266	0.219	Gumbel (G)
<b>DSM 2; Total</b>	T2	183	1.153	0.168	0.145	Lognormal (LN)
<b>DSM 3; Global Mode</b>	G3	6	1.046	0.091	0.087	Normal (N)
<b>DSM 3; Local Mode</b>	L3	163	1.035	0.112	0.109	Normal (N)
<b>DSM 3; Distortional Mode</b>	D3	14	1.144	0.240	0.210	Gumbel (G)
<b>DSM 3; Total</b>	T3	183	1.044	0.128	0.123	Lognormal (LN)
<b>DSM 4; Global Mode</b>	G4	5	1.071	0.075	0.070	Normal (N)
<b>DSM 4; Local Mode</b>	L4	138	1.043	0.114	0.110	Normal (N)
<b>DSM 4; Distortional Mode</b>	D4	40	1.078	0.171	0.158	Gumbel (G)
<b>DSM 4; Total</b>	T4	183	1.051	0.128	0.122	Lognormal (LN)
<b>DSM 5; Global Mode</b>	G5	5	1.071	0.075	0.070	Normal (N)
<b>DSM 5; Local Mode</b>	L5	146	1.055	0.117	0.111	Normal (N)
<b>DSM 5; Distortional Mode</b>	D5	32	1.073	0.189	0.176	Gumbel (G)
<b>DSM 5; Total</b>	T5	183	1.059	0.131	0.124	Lognormal (LN)

### 3. Results

The reliability indexes were calculated using the FORM, FOSM and MCM methods. The results obtained are shown in (Table 5) (Jardim, 2020). The calibration data used are derived from the AISI S100 (2016), for the following groups:

- For LRFD: (I)  $1.2D_n + 1.6L_n$ , relationship  $L_n/D_n = 5$ ,  $\phi_{LRFD} = 0.85$ .
- For LSD: (II)  $1.25D_n + 1.5L_n$ , relationship  $L_n/D_n = 3$ ,  $\phi_{LSD} = 0.80$ .

When analyzing the entire data set, it is observed that the DSM 2 option presented more conservative results, with high averages and high reliability indexes. Better values for the statistical parameters, i.e., averages close to the unit value and better coefficients of variation, were observed in the DSM 4 and DSM 5 formulations. Their reliability indexes showed very close values, due to the great similarity between the two formulations.





**Table 5.** Reliability indices for the SMC, FORM and FOSM reliability methods

Data Group	$\beta_{SMC}$			$\beta_{FORM}$			$\beta_{FOSM}$	
	LRFD	LSD	pdf	LRFD	LSD	pdf	LRFD	LSD
<b>G2</b>	2.73	2.85	N	2.76	2.87	N	2.87	3.03
<b>L2</b>	2.82	2.92	N	2.87	2.96	N	3.02	3.16
<b>D2</b>	2.80	2.85	G	2.76	2.86	G	2.71	2.79
<b>T2</b>	2.86	2.95	LN	2.85	2.96	LN	2.96	3.10
<b>G3</b>	2.72	2.90	N	2.76	2.88	N	2.88	3.04
<b>L3</b>	2.63	2.73	N	2.65	2.76	N	2.74	2.89
<b>D3</b>	2.66	2.75	G	2.62	2.71	G	2.57	2.65
<b>T3</b>	2.61	2.71	LN	2.63	2.74	LN	2.71	2.85
<b>G4</b>	2.86	2.99	N	2.89	3.02	N	3.04	3.23
<b>L4</b>	2.63	2.72	N	2.67	2.78	N	2.77	2.91
<b>D4</b>	2.66	2.77	G	2.64	2.75	G	2.65	2.76
<b>T4</b>	2.67	2.76	LN	2.66	2.76	LN	2.74	2.88
<b>G5</b>	2.86	2.99	N	2.89	3.02	N	3.04	3.23
<b>L5</b>	2.66	2.76	N	2.71	2.81	N	2.81	2.96
<b>D5</b>	2.61	2.69	G	2.56	2.66	G	2.54	2.64
<b>T5</b>	2.67	2.78	LN	2.67	2.78	LN	2.76	2.90

For MCM, 10,000 simulations were performed with the aid of Excel software. (Figure 1) and (Figure 2) show that the reliability indices calculated by the FORM method indicated a good approximation with MCM. The indices calculated by FOSM did not show a better approximation with the MCM and were, in general, superior to the others. The exceptions are the groups of distortional buckling, which showed a different pattern for the Gumbel probability distributions.

It can be seen from (Figure 1) that the reliability indices for the LRFD philosophy were higher than  $\beta_0$  of 2.5. For MCM, the  $\beta$  values range from 2.61 to 2.86, with values generally higher for the global mode. For FORM, the values range from 2.56 to 2.89, with lower  $\beta$  values for the distortional mode and generally higher  $\beta$  values for the global mode. For FOSM, the values range from 2.54 and 3.04, with lower  $\beta$  values for the distortional mode and generally higher  $\beta$  values for the global mode.

When calibration is performed from LSD data (Figure 2), with a target index  $\beta$  of 3.0, most of the results obtained are not satisfactory, with  $\beta$  predominantly lower than the target. This behavior was observed in works developed by (Ganesan, 2010); (Freitas et al., 2013) and (Capanema, 2018). The  $\beta$  values calculated by the FOSM method were those that came closest to the target.



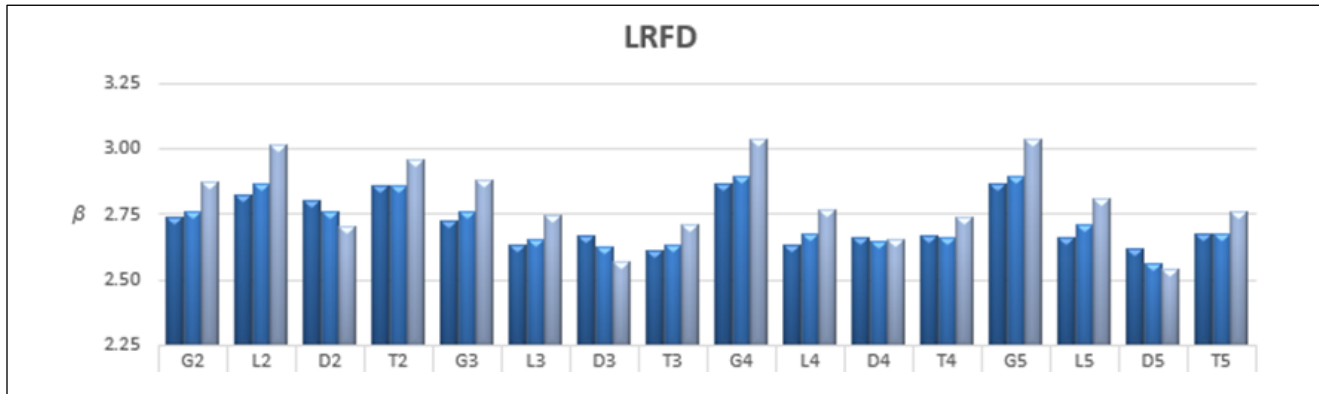


Figure 1. Reliability indices using the LRFD philosophies

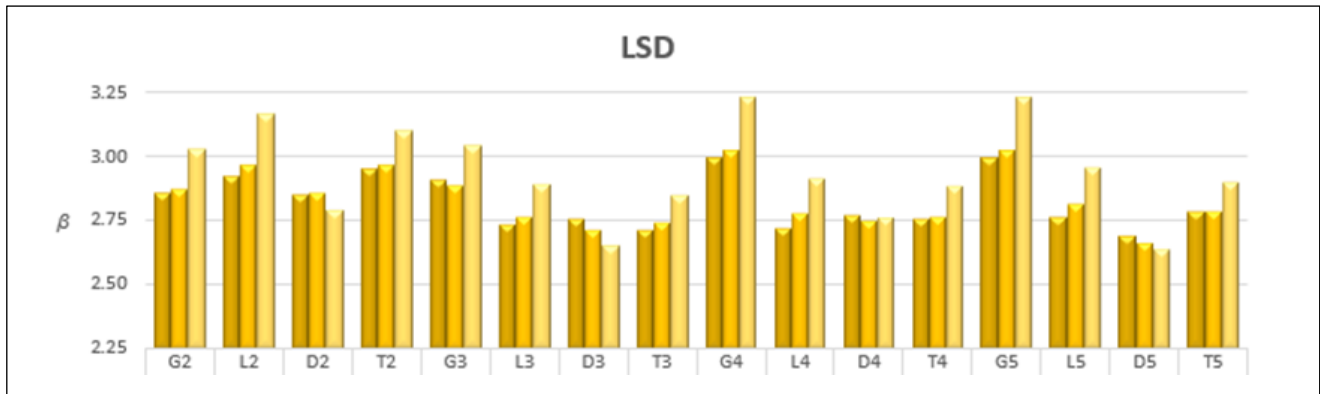


Figure 2. Reliability indices using the LSD philosophies

### 3.1 Calibration of the resistance factor

(AISI S100 2016) used the FOSM method as the basis for calibrating its standard. Resistance factors,  $\phi$ , of 0.85 and 0.8 were presented for the LRFD and LSD philosophies and profiles without perforations. In this study, the resistance factors were also obtained by the FOSM method.

(Figure 3) shows the results of the calculated resistance factors. It appears that for the LRFD philosophy, the resistance factors vary between 0.86 and 0.98, with less than  $\phi$  for the distortional buckling modes. LSD shows resistance factors varying between 0.72 and 0.84.

It appears that for the LRFD philosophy, all values were higher than those recommended by AISI for profiles without perforations. Regarding the LSD philosophy, the observed behavior is the opposite. Most of the calculated values are lower than the value presented by the standard, for profiles without perforations. These are expected behaviors when evaluating the calculated reliability indices. The distortional buckling modes also showed lower values for  $\phi$ .

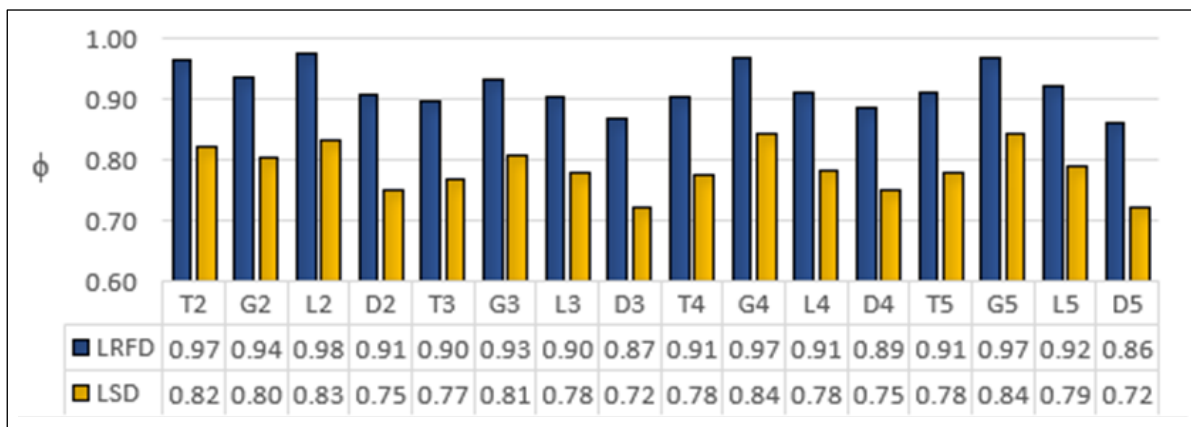


Figure 3. Resistance factors for the LRFD and LSD philosophies



## 4. Conclusions

The objective of this study was to evaluate the reliability of columns in cold-formed steel profiles with perforated webs, following the criteria proposed by (Moen and Schafer, 2008). The results obtained from this analysis allowed the following conclusions:

- The formulations DSM 4 and DSM 5 showed better results for the statistics of the professional factor.
- The DSM 2 formulation presents conservative results, with high values for the means and the reliability indices.
- For the LRFD philosophy, all data groups, regardless of the reliability method used, presented reliability indexes higher than the target  $\beta_0$  of 2.5. When  $\beta$  was set at 2.5, the results calculated for  $\phi$  were greater than 0.85, varying between 0.86 and 0.98.
- The LSD philosophy, the reliability indices did not reach the target of 3.0 in all analyzed groups. When setting  $\beta$  at 3.0, the results calculated for  $\phi$  were, in general, lower than the value adopted by the standard, with  $\phi$  equal to 0.8.

## 5. Acknowledgments

The authors would like to thank UFOP (Universidade Federal de Ouro Preto) and CAPES (Coordenação de Aperfeiçoamento de Pessoal de Nível Superior) for supporting the development of this study.

## 9. References

- Abdel-Rahman, N.; Sivakumaran, K. S. (1998)**. Effective Design Width for Perforated Cold-Formed Steel Compression Members. Canadian Journal of Civil Engineering, 25: 315–30.
- ANSI Specification. (2016). Design of Cold-Formed Steel Structural Members. American Iron and Steel Institute. Washington (DC).
- Capanema, D. C. O. (2018)**. Obtenção do Índice de Confiabilidade de Colunas de Perfis Formados a Frio com Emprego do Método FORM (Master's Thesis). Department of Civil Engineering. Ouro Preto: Universidade Federal de Ouro Preto.
- CUFSM (2020)**. CUFSM : Constrained and Unconstrained Finite Strip Method: Cross-Section Elastic Buckling Analysis. Version 4.5. Cornell University. Accessed: 20/05/2020.
- Ditlevsen, O.; Madsen, H. O. (2007)**. Structural Reliability Methods, p.361, 2ª Ed, Denmark: Department of Mechanical Engineering.
- Ellingwood, B.; Galambos, T. V.; Macgregor, J. G.; Cornell, C. A. (1980)**. Development of a Probability Based Load Criterion for American National Standard A58, U.S. Department of Commerce, National Bureau of Standards: Washington, DC.
- Freitas, M. S. R.; Brandão, A. L. R.; Freitas, A. R. (2013)**. Resistance Factor Calibration for Cold-Formed Steel Compression Members. REM-International Engineering Journal, 66: 233-238, doi: <https://doi.org/10.1590/S0370-44672013000200015>.
- Freitas, M. S. R.; Brandão, A. L. R.; Alves, A. M. S. (2018)**. Reliability Analysis of Welded and Bolted Connections in Cold-Formed Steel Sections. REM-International Engineering Journal, 71: 371-376, doi: <https://doi.org/10.1590/0370-44672016710087>.
- Ganesan, K. (2010)**. Resistance Factor for Cold-Formed Steel Compression Members (Master's Thesis). Virginia: Virginia Polytechnic Institute and State University.
- Hasofer, A. M.; Lind, N. C. (1974)**. Exact and Invariant Second-Moment Code Format. Journal of the Engineering Mechanics Division – ASCE, 100: 111-121.
- Hsiao, L. E. (1989)**. Reliability Based Criteria for Cold-Formed Steel Members (Phd Thesis). Missouri: University of Missouri-Rolla.
- Jardim, R. L. F. (2020)**. Confiabilidade de Barras com Perfurações em Perfis Formados a Frio Submetidas à Força Axial de Compressão (Master's Thesis). Ouro Preto: Universidade Federal de Ouro Preto.
- Melchers, R. E.; Beck, A. T. (2018)**. Structural Reliability Analysis and Prediction, p.506, 3ª Ed., Hoboken: John Wiley and Sons.
- Miller, T. H.; Peköz, T. (1994)**. Unstiffened Strip Approach for Perforated Wall Studs. Journal of Structural Engineering - ASCE, 120(2): 410-421.
- Moen, C. D.; Schafer, B. W. (2008)**. Direct Strength Design of Cold-Formed Steel Members with Perforations: Research Report RP 08-1. Washington: American Iron and Steel Institute – 58 Committee on Specifications for the Design of Cold-Formed Steel Structural Members.
- Moen, C. D.; Schafer, B. W. (2011)**. Direct Strength Design of Cold-Formed Steel Columns with Holes. Journal of Structural Engineering, 137(5): 559-570, doi: [https://doi.org/10.1061/\(ASCE\)ST.1943-541X.0000310](https://doi.org/10.1061/(ASCE)ST.1943-541X.0000310)
- Ortiz-Colberg R. A. (1981)**. The Load Carrying Capacity of Perforated Cold-Formed Steel Columns (Master's Thesis). Ithaca, NY: Cornell University.
- Pu, Y.; Godley, M. H. R.; Beale, R. G.; Lau, H. H. (1999)**. Prediction of Ultimate Capacity of Perforated Lipped Channels. Journal of Structural Engineering - ASCE, 125(5): 510–4, doi: [https://doi.org/10.1061/\(ASCE\)0733-9445\(1999\)125:5\(510\)](https://doi.org/10.1061/(ASCE)0733-9445(1999)125:5(510)).
- Rackwitz, R.; Fiessler, B. (1978)**. Structural Reliability Under Combined Random Load Sequences. Computers and Structures, 9(5): 489-494, doi: [https://doi.org/10.1016/0045-7949\(78\)90046-9](https://doi.org/10.1016/0045-7949(78)90046-9).
- Ravindra, M. K.; Galambos, T. V. (1978)**. Load and Resistance Factor Design for Steel. Journal of Structural Division – ASCE, 104: 1335-1354.
- Schafer, B. W.; Peköz, T. (1998, 15 October)**. Direct Strength Prediction of Cold-Formed Steel Members Using Numerical Elastic Buckling Solutions. In International Specialty Conference on Cold-Formed Steel Structures: Recent Research and Developments in Cold-Formed Steel Design and Construction (pp. 1-8). St. Louis, Missouri.
- Sivakumaran, K. S. (1987)**. Load Capacity of Uniformly Compressed Cold-Formed Steel Section with Punched Web. Canadian Journal of Civil Engineering, 14: 550–8, doi: <https://doi.org/10.1139/l87-080>.



ENGLISH VERSION.....

- Toledo, F. F. A.; Freitas, M. S. R.; Brandão, A. L. R. (2021).** Reliability Assessment of Cold-Formed Steel Beams by the FORM Method. REM – International Engineering Journal, 74(2): 183-188, doi: <https://doi.org/10.1590/0370-44672020740048>.
- Xu, L.; Shi, Y.; Yang, S. (2014, 5 November).** Compressive Strength of Cold-Formed Steel C-Shape Columns with Slotted Holes. In International Specialty Conference on Cold-Formed Steel Structures (pp. 157-170). St. Louis, Missouri: Missouri University of Science and Technology.
- Yao, X. (2017).** Experiment and Design Method on Cold-Formed Thin-Walled Steel Lipped Channel Columns with Slotted Web Holes Under Axial Compression. The Open Civil Engineering Journal, 11:244-257, doi: <https://doi.org/10.2174/1874149501711010244>.
- Yao, X.; Guo, Y.; Nie Z. (2016, 9 November).** Distortional Buckling Experiment on Cold-Formed Steel Lipped Channel Columns with Circle Holes Under Axial Compression. In International Specialty Conference on Cold-Formed Steel Structures (pp. 187-202). Baltimore, Maryland: Missouri University of Science and Technology.

